Mineralogy and Petrology (2003) 78: 231–241
DOI 10.1007/s00710-002-0226-z

Mineralogy and Petrology
Printed in Austria

Trace hydrogen zoning in diopside

M. Andrut[1], **F. Brandstätter**[2], and **A. Beran**[1]

[1] Institut für Mineralogie und Kristallographie, Universität Wien-Geozentrum, Austria
[2] Mineralogisch-Petrographische Abteilung, Naturhistorisches Museum, Wien, Austria

Received July 11, 2002; accepted October 30, 2002
Published online February 24, 2003;
Editorial handling: E. Tillmanns

Summary

The trace hydrogen content of a colourless to light-green zoned diopside single-crystal from Zillertal was investigated by IR microspectroscopy. The light-green part of the crystal reveals pleochroic OH absorption bands centred at 3645, 3463, and 3358 cm^{-1} which are attributed to structural OH defects. The OH absorptions of the colourless crystal part are characterised by weak bands at 3645 and 3662 cm^{-1} and by a strong band at 3676 cm^{-1}. The bands at 3662 and 3676 cm^{-1} are attributed to the presence of amphibole lamellae. The analytical water content due to the structural OH defect concentration of the light-green crystal part amounts to 0.0016 wt.%, that of the colourless part is lowered by a factor of about 50. According to optical absorption spectra, the light-green colour of the crystal is essentially caused by an Fe^{2+}–Fe^{3+} charge transfer. The relatively high concentration of OH defects in the light-green crystal part associated with higher Al contents relative to the colourless part suggests that OH is incorporated as "*hydrodiopside*" component, $CaMg(SiAlO_5OH)$. It is concluded that increasing water activity during the crystallisation process causes the formation of amphibole lamellae under consumption of nearly all of the water available in the fluid phase. It is further concluded that the observed hydrogen content of diopside represents a primary incorporation and not the result of late hydrothermal alteration processes.

Introduction

Most pyroxenes contain significant amounts of hydrogen in the form of hydroxyl groups with concentrations ranging from about 100 to 1300 wt.ppm H_2O (*Skogby* et al., 1990; *Smyth* et al., 1991; *Bell* and *Rossman*, 1992; *Ingrin* and *Skogby*, 2000). Pyroxene may indeed be the main storage site for hydrogen in the Earth's upper mantle. However, the measured water content indicates the amount of water

preserved in the mineral phase. Hydrogen exchange with magma and hydrogen degassing are related processes which could occur during ascent of the pyroxenes from the mantle (*Ingrin* et al., 1995). The insensitivity of hydrogen solubility on temperature for samples that were rapidly quenched by eruption or recovered from low-temperature hydrothermal conditions suggest the use of the hydrogen concentration as an independent pH_2 meter (*Hercule* and *Ingrin*, 1999).

Skogby et al. (1990) showed that hydrogen concentration in pyroxenes vary as a function of geological environment with the greatest amounts occurring in mantle derived samples. It is suggested that also crystal chemical or compositional factors control the incorporation of trace hydrogen. *Hercule* and *Ingrin* (1999) proposed that hydrogen incorporation in Fe bearing crystals, following the reaction $Fe^{3+} + O^{2-} + 1/2\ H_2\ (g) = Fe^{2+} + OH^-$ (*Ingrin* et al., 1989; *Skogby* and *Rossman*, 1989), is rate-limited by the mobility of electron holes connected with the Fe oxidation–reduction process. It is further proposed that the kinetics of hydrogen uptake in clinopyroxene will increase with increasing Fe content until it is rate-controlled by the kinetics of hydrogen self-diffusion.

Infrared (IR) spectroscopy provides an extremely sensitive method for detecting trace hydrogen bonded to oxygen, thus forming OH defects in the structure of various nominally anhydrous minerals (*Rossman*, 1990; *Beran*, 1999; *Ingrin* and *Skogby*, 2000). Polarised IR spectroscopic studies of diopsides from different localities revealed two types of OH absorption bands with opposite pleochroic behaviour, conventionally denoted group I bands (absorptions around $3640\,cm^{-1}$) and group II bands (absorptions around 3535, 3460 and $3355\,cm^{-1}$). In most spectra of diopsides the band at $3460\,cm^{-1}$ is the strongest. The two types of bands suggest that at least two types of OH positions exist simultaneously in the diopside structure (*Beran*, 1976; *Ingrin* et al., 1989; *Skogby* and *Rossman*, 1989; *Skogby* et al., 1990). Based on the pleochroism of the $3640\,cm^{-1}$ band, *Beran* (1976) proposed a model for the hydrogen incorporation into the structure of diopside with OH groups partially replacing the O2 ''zigzag'' oxygens and pointing to the O3 ''chain'' oxygen of a neighboured silicate chain. Further structural information is evaluated from the number of OH vibrations and from the band energies, as these depend on the local environment of the OH defects and on hydrogen bond lengths and strengths. The position and pleochroism of the absorption bands are similar for different samples, but the absolute intensities vary strongly. Integrated IR absorbances (A_i) of polarised measurements are directly related by the integrated molar absorption coefficient (ε_i) to the concentration of the OH groups (c) and to the thickness of the samples (t). This relation is expressed by Beer's law $A_i = \varepsilon_i * c * t$; accordingly, the hydrogen concentration can only be determined if the matrix specific molar absorption coefficient is known. A clinopyroxene megacryst characterised by group I and II bands at 3625, 3540, and $3460\,cm^{-1}$ was analysed by *Bell* et al. (1995) using H_2 manometry and its integrated molar absorption coefficient was determined to be $\varepsilon_i = 38300 +/- 17001 * mol^{-1}{}_{H_2O} * cm^{-2}$. This ε_i value is close to that calculated from the calibration curve of *Libowitzky* and *Rossman* (1997).

In the present study we have investigated the concentration profile of hydrogen in a natural hydrothermally formed diopside single-crystal showing a distinct colour zoning. The aim of this work is to establish the relationship between the OH

concentration and compositional factors, in particular the presence of Fe, and to argue whether the hydrogen concentration can provide information about the activity of a hydrous component during the crystallisation process.

Experimental

Sample

The Alpine fissures in ultramafic rocks located close to Ochsner and Rotkopf, Oberer Zemmgrund, Zillertal, Tirol, Austria are a famous locality for light- to dark-green coloured diopsides of gem-quality. An elongated single-crystal, ca. $15 * 3 * 2$ mm in size, dominated by the (100) face, colourless at one end and light-green at the other end was selected as a typical variety and used for the detailed measurements. The sharply contrasting colourless zone comprises approximately one third of the crystal which is schematically represented in Fig. 1. Additional diopside crystals were used for additional spectroscopic measurements.

Under the optical microscope the selected gem-quality samples proved to be largely free of inclusions and impurities. Sample preparation consisted of

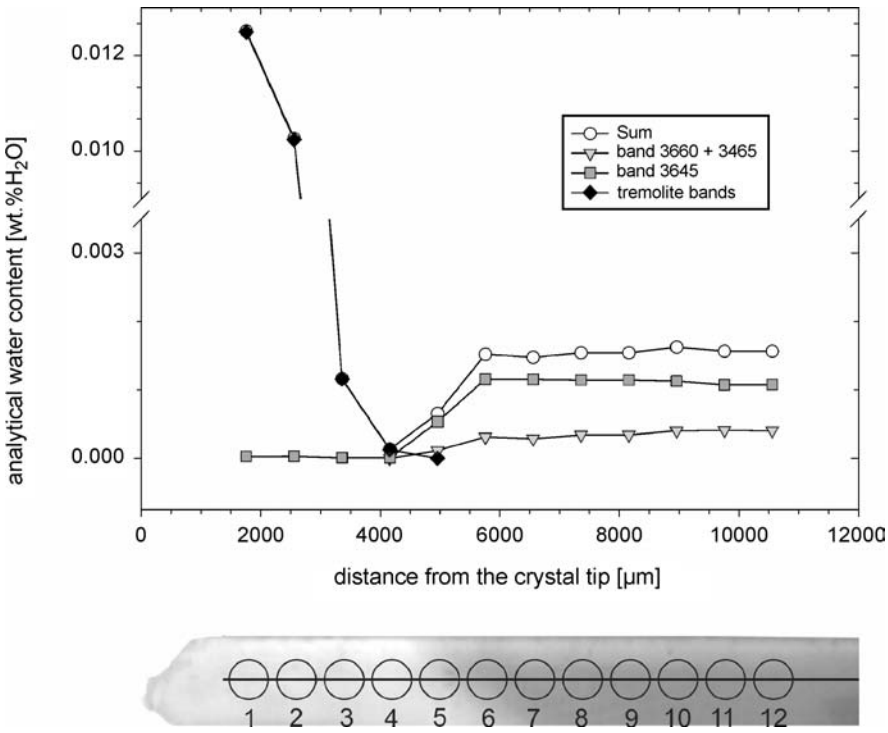

Fig. 1. Drawing of the colour zoned diopside single-crystal from Zillertal, Austria, dominated by the (100) face. The greyish hue represents the light-green colour. The area measured by IR spectroscopy is indicated by circles (numbers 1–12) and the corresponding OH defect concentration is plotted as analytical H_2O values; the continuous line corresponds to the microprobe profile with measuring points in a distance of 50 µm

orienting the crystal by morphology and optical methods, followed by preparing two plane-parallel, self-supporting crystal slabs. The first series of IR measurements and microprobe analyses was performed on a slab polished parallel (100); successively this slab was cut parallel (010) in two pieces by the use of a low-speed diamond saw, and a second series of measurements was performed on one of these newly produced slabs. The profiles of the unpolarised IR spectroscopic and microprobe measurements on (100) parallel to the c direction are indicated in Fig. 1.

Analytical and spectroscopic methods

Chemical analyses of the diopside slabs were performed with an automated ARL-SEMQ electron microprobe at 15 kV operating voltage and 15 nA sample current measured on benitoite. The analyses were corrected by the modified correction procedures of *Armstrong* (1984) and *Love* and *Scott* (1978). Standards used were augite (Ca, Mg), garnet (Si, Al, Fe), jadeite (Na), kaersutite (Ti), and tephroite (Mn).

Unpolarised and polarised single-crystal spectra were recorded from 3900 to 2900 cm^{-1} with a Bruker FTIR spectrometer IFS 66v/S which was equipped with a liquid nitrogen-cooled MCT detector and a KRS-5 wire grid polarizer. 250 scans were averaged for each spectrum, nominal resolution was 1 cm^{-1}. Because of the relatively large dimension of the clear parts of the crystal, the diameter of the beam was chosen to 800 µm for the profile scans and 300 µm for the polarised measurements, respectively.

Optical spectra were recorded from 35000 to 15000 cm^{-1} and from 20000 to 5000 cm^{-1} with a calcite Glan-prism polarising Bruker IRscope II microscope combined with the Bruker FTIR spectrometer IFS 66v/S. Spectra were averaged over 2048 scans, the spectral band width was 20 cm^{-1}. Appropriate combinations of light sources (tungsten lamp, Xe lamp) and detectors (Si diode, Ge diode, GaP diode) were used. The spectra recorded with different instrumental configurations were fitted together and displayed as linear absorption coefficients $\alpha = A/t$, where A denotes the linear absorbance.

Results

A series of unpolarised OH absorption spectra measured on the (100) face of the diopside sample from Zillertal is shown in Fig. 2. The results of these measurements were confirmed by a second series of measurements on (010). The light-green part of the crystal reveals OH absorption spectra with bands centred at 3645, 3463, and 3358 cm^{-1} which are comparable to those reported in the literature (*Ingrin* et al., 1989; *Skogby* et al., 1990; *Smyth* et al., 1991). The band at 3645 cm^{-1} is assigned to group I, the 3463 and 3358 cm^{-1} bands are assigned to group II. The full width at half height (FWHH) of the bands is in the order of 30 cm^{-1}. The band intensities are varying within a limited range. In the spectral range 3600–3500 cm^{-1} a system of strongly overlapping bands is observed. Due to their weak intensity and the insignificant pleochroic behaviour, these bands will be not discussed any further. Overtones are located at 7353 and 6980 cm^{-1}.

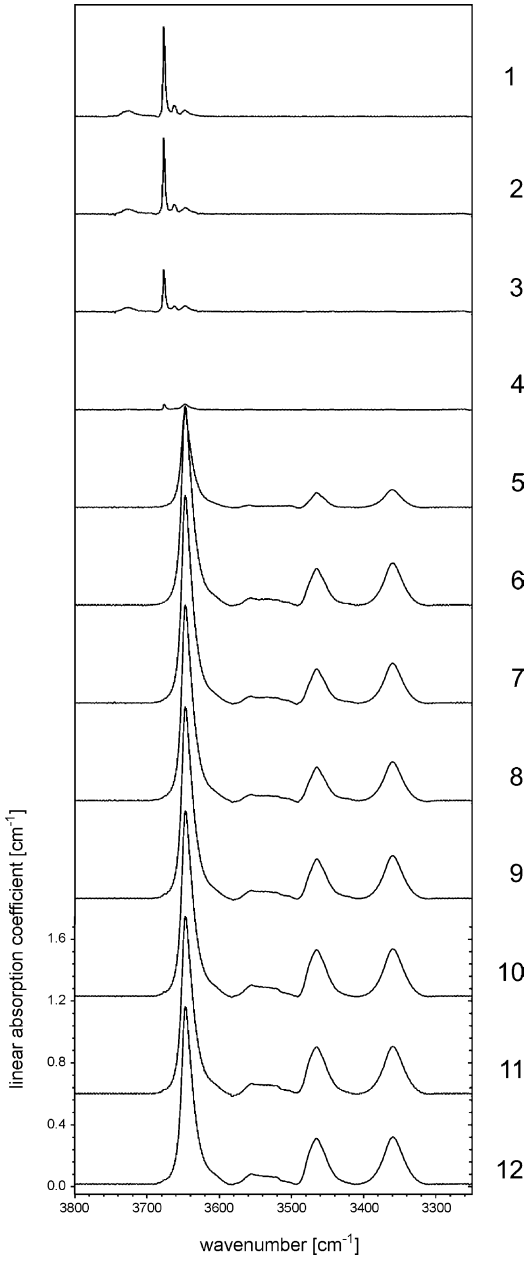

Fig. 2. Unpolarised OH absorption spectra of diopside measured on (100) along the profile indicated in Fig. 1. The weak intensities of the tremolite bands at 3676 and 3662 cm^{-1} are due to the strong polarisation effect of the oriented intergrown amphibole lamellae

Polarised spectra were measured parallel to the main axes of the optical indicatrix, where n_α is close to the maximum absorption of the most intense band at 3645 cm^{-1} (*Beran*, 1976; *Ingrin* et al., 1989). The polarised spectra of a distinct sample area within the light-green crystal part are shown in Fig. 3.

The OH absorptions of the colourless crystal part reveal a completely different type of spectrum, characterised by weak bands at 3645 and 3662 cm^{-1} and by an additional, very strong band at 3676 cm^{-1} (Fig. 2). The bands at 3676 and 3662 cm^{-1} exhibit a FWHH of 5 cm^{-1} and show an identical pleochroism. The

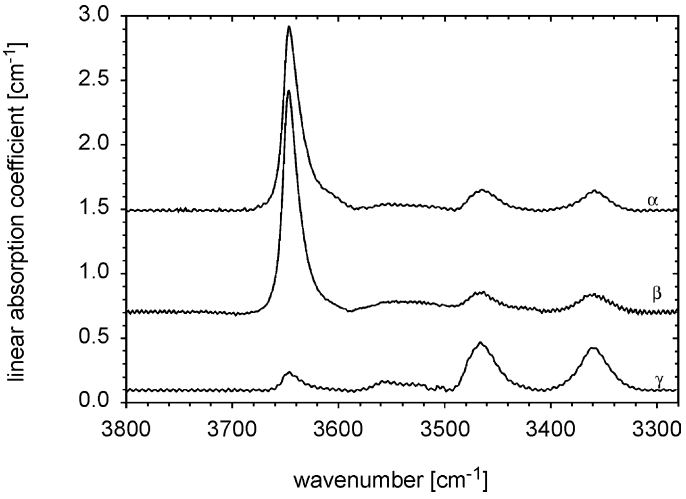

Fig. 3. Polarised OH absorption spectra, typical for the light-green crystal part, measured parallel to the axes of the optical indicatrix

band at 3645 cm^{-1} is significantly broader and its pleochroic behaviour deviates from that of the bands at 3676 and 3662 cm^{-1}. The occurrence of a weak band around 3730 cm^{-1} is related to the presence of the two sharp bands. Spectra from colourless samples could also be observed without showing bands at 3676, 3662, and 3730 cm^{-1}. In some samples a weak absorption band at 3489 cm^{-1} is present, revealing a pleochroic behaviour which corresponds to that of the 3645 cm^{-1} band. An overtone is observed at 7295 cm^{-1}.

Evaluating the analytical H_2O content on the basis of Beer's law, the most intense absorption spectrum of the light-green crystal part, which corresponds to measuring point 10 in Fig. 1, was used for the determination of the integrated absorbance values by integrating over the entire spectral region from 3700 to 3300 cm^{-1}. The integrated absorbance values, measured parallel to the axes of the optical indicatrix (Fig. 3) were summed up to obtain the total integrated absorbance values. Using the integrated ε_i value of $38300\,l * mol^{-1}{}_{H_2O} * cm^{-2}$ (*Bell* et al., 1995), the analytical H_2O content of point 10 was calculated to be 17.7 wt.ppm. For comparison, the total integrated absorbance values were also determined for the individual bands centred at 3645, 3463, and 3358 cm^{-1}. The respective ε_i values, derived from the calibration curve of *Libowitzky* and *Rossman* (1997), were used for the calculation of the H_2O content related to each band. The total analytical H_2O content derived from all individual bands yielded 16.2 wt.ppm. This value is very close to that determined by using the integrated ε_i value of *Bell* et al. (1995) based on the manometric H_2 analysis. However, despite the good agreement between these two sets of extinction coefficients, it should be noted that the bands in the clinopyroxene spectra of *Bell* et al. (1995) are in parts located in a different spectral region compared to our sample and that the authors derived only one ε_i value for the H_2O content that originates from separated bands. Significant errors will be undoubtedly introduced in case of samples covering a different spectral region and/or intensity distribution compared to the sample used by *Bell* et al. (1995). We decided to use the individual values of the different bands to standardise the unpolarised measurements giving the values for the H_2O content

plotted in Fig. 1. The summed mean OH band absorbances of the colourless crystal part are weaker by a factor of about 50 than those of the light-green crystal part, indicating an essentially lower structural hydrogen incorporation in the colourless part of the diopside crystal.

Polarised optical absorption spectra were recorded on a (100) slab parallel to [001] and parallel to [010], i.e. n_β and are shown in Fig. 4. Absorption bands at around 11000 and 8000 cm^{-1} are assigned to Fe^{2+} in M1, bands around 9500 and 4500 cm^{-1} are assigned to Fe^{2+} in M2 (*Rossman*, 1980). The colourless part of

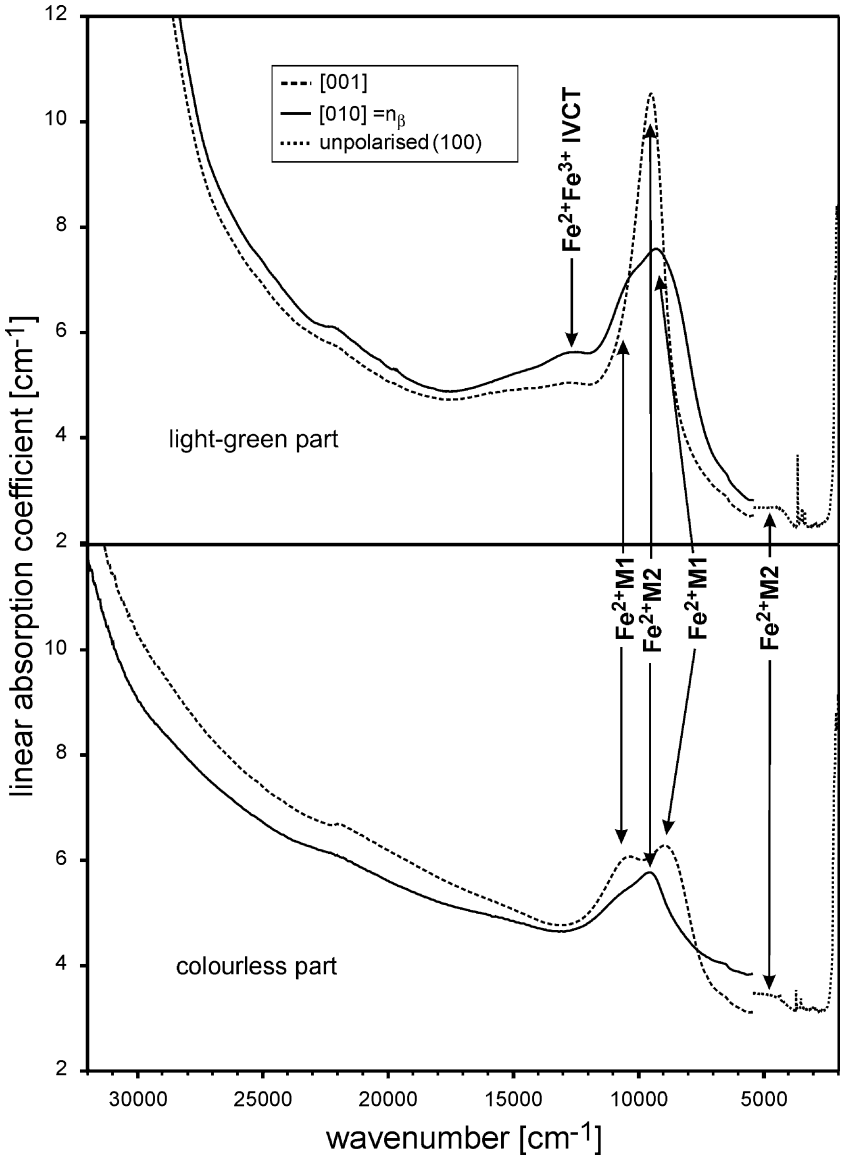

Fig. 4. Optical absorption spectra measured parallel [001] and [010], i.e. n_β in the light-green and in the colourless part of the diopside crystal

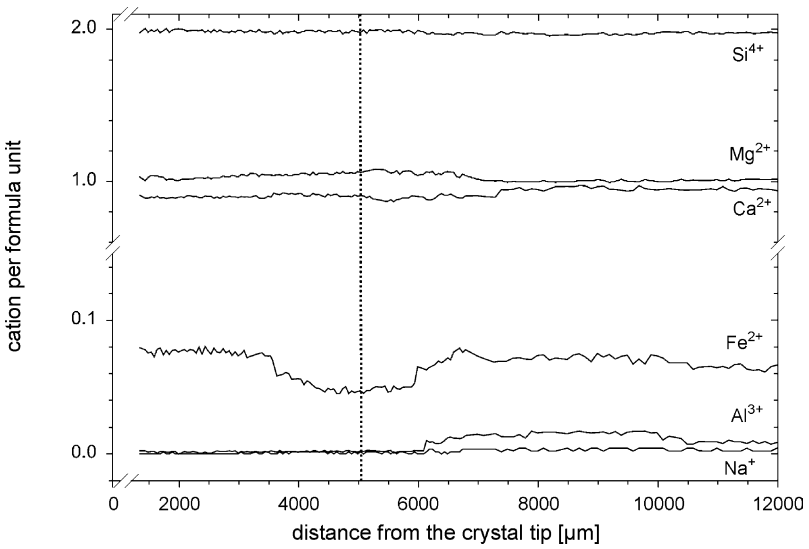

Fig. 5. Profiles of microprobe measurements along the path indicated by the continuous line in Fig. 1. Note the different ordinate scales. Vertical dotted line divides the light-green from the colourless crystal part. Distance of the individual measuring points 50 µm

the crystal reveals only transitions which are due to Fe^{2+} in M1, whereas the light-green part exhibits both, transitions due to Fe^{2+} in M1 and in M2. Weak absorptions around 12600 cm^{-1} in the light-green crystal part are caused by Fe^{2+}–Fe^{3+} intervalence charge transfer (IVCT). These data are in agreement with results obtained on hedenbergite by *Amthauer* and *Rossman* (1984) and ferrian diopside by *Skogby* and *Rossman* (1989).

Profiles of microprobe measurements are presented in Fig. 5. The colourless crystal part is subdivided by the Fe content showing significantly higher values at the upper end of the crystal. Within the colourless part the Mn content, ranging from about 0.015 to 0.005 cation pfu, is positively correlated with Fe and, in contrast to Fe, remaining at low values also in the light-green part. Ca shows a negative correlation with Fe and Mn in the colourless part and increased values in the light-green part. Mg slightly increases within the colourless part of the crystal and reveals a decrease at the colour dividing line, followed by constant but lower values in the light-green crystal part. This behaviour results in a negative correlation of Mg with Al and Na. The Na content is close to the detection limit of the microprobe but shows a significant enhancement within the coloured part, that is also characterised by significantly lower Si values. The highest Al content is observed in a zone adjacent to the colourless part but the Al values remain essentially enhanced along the microprobe profile within the light-green part. The Fe content of the light-green part is similar to that prevailing in the upper colourless crystal part.

The results of the IR spectroscopic and microprobe measurements obtained on the (100) section were completely confirmed by the second series of measurements performed on the (010) section.

Discussion

The results of optical absorption spectroscopy clearly demonstrate that in the light green part some Fe is present in the trivalent state. As stated by *Skogby* and *Rossman* (1989) on the basis of Mössbauer spectroscopy for ferrian diopside, Fe^{3+} is also located in tetrahedral coordination. One may speculate whether small amounts of tetrahedrally coordinated Fe^{3+} are also present in the light-green part of diopside which shows significantly lower Si values. Fe^{2+} is distributed between the M1 and M2 site of the diopside structure. As evident from the band intensities, in the light-green part of the crystal more Fe^{2+} is fractionated into the M2 position than in the colourless part. The light-green colour is caused by absorption due to Fe^{2+}–Fe^{3+} IVCT.

The significantly enhanced Na content along with the high Al content of the light-green crystal part are indicative for a jadeite component. In coincidence with a significantly lower Si content, with slightly lower Mg values, and with the constant, even slightly enhanced Ca values, most of the Al is ascribed to a $CaAl(SiAlO_6)$ *tschermakite* component. In addition, the relatively high concentration of OH defects combined with the high Al content in the light-green part of the crystal suggests the presence of a *"hydrodiopside"* component, $CaMg(SiAlO_5OH)$, to provide charge balance. As shown by *Beran* (1976), a model for the OH defect incorporation can be developed on the basis of the pleochroic scheme for the prominent band at 3645 cm^{-1}, without assuming changes of the ideal structural arrangement. However, charge compensation for OH groups replacing O atoms can also be provided by vacancies on the Si or M sites of the structure.

The light-green part of our diopside crystal shows an OH absorption spectrum which is comparable with literature data on diopsides from different localities and geological environments (*Skogby* et al., 1990; *Smyth* et al., 1991). As a specific feature, the group I band at 3645 cm^{-1} is the most intense of the spectra and its intensity is strongly decreasing near the contrasting, colour dividing line of the crystal. In the colourless part this band is still present but with extremely low intensities. The relatively weak group II bands in the light-green part centred at 3463 and 3358 cm^{-1} are completely absent in the colourless crystal part. The colourless diopside reveals quite different OH absorption properties. The dominating sharp band doublet at 3676 and 3662 cm^{-1} as well as the weak absorption around 3730 cm^{-1} are attributed to the presence of amphibole lamellae in the colourless diopside. According to the OH band assignment for amphiboles of *Burns* and *Strens* (1966), the band doublet is related to the coordination of the OH groups by the three divalent cations on M1,3 sites, while the OH dipole points to a vacant A site. In particular, the main band at 3676 cm^{-1} is assigned to three Mg atoms at the M sites sharing the proton carrying oxygen as a ligand. The 3662 cm^{-1} band is assigned to OH coordinated by two Mg and one Fe. The relative integrated band intensities indicate an amphibole composition close to the tremolite end member. The weak absorption around 3730 cm^{-1} consists of two partly superimposing components at 3724 and 3733 cm^{-1}, which are assigned to amphibole bands with an alkaline ion occupying the A site (*Rowbotham* and *Farmer*, 1973; *Hawthorne* et al., 1997; *Gottschalk* and *Andrut*, 1998). Due to the repelling force of the alkaline ion on the OH dipole, the stretching vibrational

frequency is shifted to higher wavenumbers. These observations are in agreement with the TEM study of *Ingrin* et al. (1989), proving the presence of clinoamphibole lamellae in an ''Austrian diopside'' and with the FTIR spectroscopic study of *Skogby* and *Rossman* (1989) which shows sharp ''amphibole'' bands around 3670 cm^{-1} in some pyroxenes from different localities.

A weak band centred at 3489 cm^{-1} with a pleochroic behaviour similar to that of the 3645 cm^{-1} band can be observed in some colourless diopsides and probably represents an additional type of OH defect. Despite its similar pleochroic behaviour with the group I band, this absorption lies within the lower energetic band group II.

The different types of OH defects in pyroxenes are controlled by the coordinating cation sites or even vacant sites and consequently by compositional variations. However, no indication exists for an expected correlation between the hydrogen content and the Fe content. Despite the fact that the hydrogen concentrations of the colourless part differ by more than one order of magnitude from those of the light-green crystal part, only slight changes in the Fe contents were observed. Evidently, the presence of amphibole as a hydrous mineral phase strongly reduces the incorporation of hydrogen into the structure of diopside. From this observation it is concluded that changing conditions of increasing water activity during the crystallisation process cause the formation of amphibole under consumption of nearly all of the water available in the fluid phase. It should also be noted that diopside forms at low p/T hydrothermal conditions that correspond to those of low grade metamorphism. Diopside disappears at intermediate metamorphic grades and then reappears at high-grade metamorphism (*Spear*, 1995). It is further concluded that the observed OH concentrations in the light-green crystal part represent maximum values which can be incorporated in hydrothermally formed diopside. These observations suggest that the determined hydrogen content is the result of a primary OH incorporation into the structure and not of a late secondary alteration process. However, these results show that hydrogen concentrations are controlled not only by the chemical composition of the host mineral, but also by the amount of water available during crystallisation. Therefore, hydrogen concentrations in dry mineral systems could be used as an indicator for the water activity prevailing during the formation of the crystal.

Acknowledgements

Thanks are due to *A. Wagner* for the careful sample preparation. This study was financially supported by the European Commission through the programme ''Human Potential-Research Training Networks'' No. RTN1-1999-00353. We gratefully acknowledge the constructive comments of two anonymous reviewers, helping to improve the manuscript.

References

Amthauer G, Rossman GR (1984) Mixed valence of iron in minerals with cation clusters. Phys Chem Minerals 11: 37–51

Armstrong JT (1984) Quantitative analysis of silicate and oxide minerals: a reevaluation of ZAF corrections and proposal for new Bence-Albee coefficients. In: *Romig AD,*

Goldstein JI (eds) Microbeam analysis. San Francisco Press, San Francisco, pp 208–212

Bell DR, Rossman GR (1992) Water in Earth's mantle: the role of nominally anhydrous minerals. Science 255: 1391–1397

Bell DR, Ihinger PD, Rossman GR (1995) Quantitative analysis of trace OH in garnet and pyroxenes. Am Mineral 80: 465–474

Beran A (1976) Messung des Ultrarot-Pleochroismus von Mineralen. XIV. Der Pleochroismus der OH-Streckfrequenz in Diopsid. Tschermaks Mineral Petrogr Mitt 23: 79–85

Beran A (1999) Contribution of IR spectroscopy to the problem of water in the Earth's mantle. In: *Wright K, Catlow R* (eds) Microscopic properties and processes in minerals. Kluwer, Dordrecht, pp 523–538

Burns RG, Strens RGJ (1966) Infrared study of the hydroxyl bands in clinoamphiboles. Science 153: 890–892

Gottschalk M, Andrut M (1998) Structural and chemical characterization of synthetic (Na, K)-richterite solid solutions by EMP, HRTEM, XRD and FTIR-spectroscopy. Phys Chem Minerals 25: 101–111

Hawthorne FC, Della Ventura G, Robert J-L, Welch MD, Raudsepp M, Jenkins DM (1997) A Rietveld and infrared study of synthetic amphiboles along the potassium-richterite-tremolite join. Am Mineral 82: 708–716

Hercule S, Ingrin J (1999) Hydrogen in diopside: diffusion, kinetics of extraction-incorporation, and solubility. Am Mineral 84: 1577–1587

Ingrin J, Skogby H (2000) Hydrogen in nominally anhydrous upper-mantle minerals: concentration levels and implications. Eur J Mineral 12: 543–570

Ingrin J, Latrous K, Doukhan J-C, Doukhan N (1989) Water in diopside: an electron microscopy and infrared spectroscopy study. Eur J Mineral 1: 327–341

Ingrin J, Hercule S, Charton T (1995) Diffusion of hydrogen in diopside: results of dehydration experiments. J Geophys Res 100: 15,489–15,499

Libowitzky E, Rossman GR (1997) An IR absorption calibration for water in minerals. Am Mineral 82: 1111–1115

Love G, Scott VD (1978) Evaluation of a new correction procedure for quantitative electron microprobe analysis. J Phys D18: 1369–1376

Rossman GR (1980) Pyroxene spectroscopy. In: *Prewitt CT* (ed) Pyroxenes. Rev Mineral 7: 93–115

Rossman GR (1990) Hydrogen in ''anhydrous'' minerals. Nuclear Instr Meth Phys Res B45: 41–44

Rowbotham G, Farmer VC (1973) The effect of ''A'' site occupancy upon hydroxyl stretching frequency in clinoamphiboles. Contrib Mineral Petrol 38: 147–149

Skogby H, Rossman GR (1989) OH^- in pyroxene: an experimental study of incorporation mechanisms and stability. Am Mineral 74: 1059–1069

Skogby H, Bell DR, Rossman GR (1990) Hydroxide in pyroxene: variations in the natural environment. Am Mineral 75: 764–774

Smyth JR, Bell DR, Rossman GR (1991) Incorporation of hydroxyl in upper-mantle clinopyroxenes. Nature 351: 732–735

Spear FS (1995) Metamorphic phase equilibria and pressure-temperature-time paths. Mineral Soc Am Monogr: 469–489

Authors' addresses: *M. Andrut* and *A. Beran* (corresponding author), Institut für Mineralogie und Kristallographie, Universität Wien-Geozentrum, Althanstrasse 14, A-1090 Wien, Austria, e-mail: anton.beran@univie.ac.at; *F. Brandstätter*, Mineralogisch-Petrographische Abteilung, Naturhistorisches Museum, Burgring 7, A-1010 Wien, Austria